





Processing-induced residual stresses in TWIP steel weld spots

Tiago C. A. Colombo, Ronnie Rego, Alfredo R. de Faria & Jorge Otubo


To cite this article: Tiago C. A. Colombo, Ronnie Rego, Alfredo R. de Faria & Jorge Otubo (2020) Processing-induced residual stresses in TWIP steel weld spots, Materials and Manufacturing Processes, 35:5, 572-578, DOI: [10.1080/10426914.2020.1734619](https://doi.org/10.1080/10426914.2020.1734619)

To link to this article: <https://doi.org/10.1080/10426914.2020.1734619>

 View supplementary material [↗](#)

 Published online: 09 Mar 2020.

 Submit your article to this journal [↗](#)

 Article views: 102

 View related articles [↗](#)

 View Crossmark data [↗](#)
CrossMark



Processing-induced residual stresses in TWIP steel weld spots

Tiago C. A. Colombo^a, Ronnie Rego^a, Alfredo R. de Faria^a, and Jorge Otubo^{b,c}

^aCompetence Center in Manufacturing, Aeronautics Institute of Technology (ITA), São José Dos Campos, Brazil; ^bMechanical Engineering Division, Aeronautics Institute of Technology (ITA), São José dos Campos, Brazil; ^cNuclear and Energy Research Institute (IPEN/CNEN), São Paulo, Brazil

ABSTRACT

The present study investigates the evolution of the residual stresses in TWIP steels induced by manufacturing chain for the production of automotive body-in-white. Two different manufacturing routes were considered. The first route encompassed a plastic deformation prior to the welding stage, whereas the second involved the spot welding followed by a baking treatment. A convergent approach was adopted to isolate the effects of the first and final manufacturing steps. The findings showed that the plastic deformation prior to the welding stage is not annihilated by the welding thermomechanical cycle. Abrupt hardness gradients along small material fractions are observed. The residual stresses state changes, although its profile is still defined by the welding stage. The post-weld bake treatment showed to promote slight residual stresses relaxation, but it is not effective in inducing the same post-weld residual stresses state for different RSW parameters set.

ARTICLE HISTORY

Received 24 January 2020
Accepted 18 February 2020

KEYWORDS

TWIP; manufacturing; chain; residual; stresses; resistance; spot; welding; RSW; body-in-white; advanced; high; strength; steels; AHSS; XRD

Introduction

In an automotive body-in-white (BIW) manufacturing chain, the working materials are prone to numerous changes of shape and properties. The main transformation stages are the stamping, the assembly of the individual stamped parts and a post-assembly paint-baking treatment. Considering the stamping stage, the Twinning-Induced Plasticity (TWIP) steels are high potential candidates for large-scale applications in the automotive architecture, mainly as cold stampable replacement materials for conventional mild steels and hot stamping steels. As stated by De Cooman et al.^[1], the versatile properties that TWIP steels exhibit are due to the nucleation and growth of mechanical twins during the plastic deformation, which enhances a high work hardening rate at the same time that favors ductility. Zavattieri et al.^[2] reported that TWIP steels undergo inhomogeneous plastic deformation during the stamping processes. According to Withers and Bhadeshia^[3], inhomogeneous plastic deformation and mechanical twinning are primary sources for residual stresses.

The assembly of the stamped parts is commonly made by means of welding processes, being the resistance spot welding (RSW) the most applied technique.^[4] The RSW cycle may induce residual stresses in TWIP steels from at least three different sources: inhomogeneous plastic deformation due to the thermomechanical cycle, mechanical twinning generated by the plastic deformation and by the action of the welding electrodes and material mismatches due to the inhomogeneous distribution of strain hardening along the weld spots. The sensitivity of the residual stresses in TWIP steels to the RSW parameters is evidenced in the study of Colombo et al.^[5] Their findings suggest that the residual stresses induced by the

RSW stage are predominantly tensile stresses along the surface of the weld spots, and they are directly correlated to the hardness distributions along the weld spots, which are controlled by the welding parameters.

Following the shaping and welding stages, the assembled components in a BIW manufacturing chain undergo a paint-baking treatment (BT). It is a thermal cycle at temperatures normally ranging between 150–240°C for up to 1 h. Although the temperatures involved in the BT are considered low for steels, the microstructure and mechanical properties of TWIP steel and other AHSS are sensitive to this process, as verified by Kilic et al.^[6]

Each of the steps throughout a manufacturing chain leaves traces in the form of residual stresses in the working material to preserve the equilibrium principle. The importance of understanding the influence of the manufacturing chain is reflected on the increase of scientific publications dedicated to the topic. Recently, Rego et al.^[7] showed that final surface integrity of gears is defined by the interaction between individual steps along the manufacturing chain, by means of a concept of “Unstable Area of Residual Stresses”.

Due to the numerous sources for residual stresses along a BIW manufacturing chain involving TWIP steels (e.g. inhomogeneous plastic deformation, displacive transformations, inhomogeneous distributions of material properties, etc.), it is also expected that the residual stresses state may be significantly altered not only by variations in the RSW parameters, but also by variations in the individual stages throughout the entire manufacturing chain. Under the perspective of a broader use of TWIP and other Advanced High-Strength Steels in the automotive architecture, it is thus necessary to understand the

role of each individual manufacturing stage on the final residual stresses state in weld spots involving such materials.

The objective of the present study is to investigate the effects of the manufacturing chain on the residual stress state of TWIP steel weld spots. The approach includes two experimentally investigated manufacturing routes, one involving a manufacturing stage prior to the RSW and another considering a post-weld manufacturing stage. The approach includes the comparison to the residual stresses induced solely by the welding process. Changes in material features along the weldment and their correlation to the residual stresses state are discussed. The main contributions lie in bringing experimental evidences for the relevance of considering the entire manufacturing chain to a more assertive comprehension of the integrity of TWIP steel weld spots.

Materials and methods

Uncoated cold rolled 0.8 mm thick Fe-16.4Mn-0.75 C-1.9Al (in wt.%) austenitic TWIP steel sheets with an initial average grain size of 2.5 μm were considered in this study. The steel sheets were water jet cut in 50 mm length by 30 mm width oriented in the rolling direction.

The experimental scope was conceived in order to follow a convergent structure. Samples were produced by varying the parameters of the first processing stage and then subjected to a same second process in the investigated manufacturing route. It effectively enables to identify the effects of a prior processing stage on the integrity state induced by the subsequent processes. A convergent structure also allows to identify the relevance of earlier processing stages on the final integrity state. Starting from the as-rolled sheets, two distinct manufacturing routes were considered. The first one involved a plastic deformation (stretching – ST) followed by the RSW as the final process (referred to as ST+RSW), in order to simulate

a manufacturing chain contemplating the forming (stamping) stage. It aims to identify the influence of the prior plastic stretching to the weld spot integrity. The second case involved the RSW plus an additional annealing stage to simulate a baking treatment as the final process (referred to as RSW+BT). Analogously, it is expected to observe how much the heat treatment reproduces the integrity state produced by the previous welding process. Fig 1 summarizes the manufacturing routes. The integrity of the weld spots considering solely the resistance spot welding process (referred to as RSW), with no additional interferences, is used for comparison.

The individual sheets were welded under a linear overlapping setup, as shown in Fig. 2a. A pair of truncated class 2 copper electrodes with a face diameter of 6.0 mm with constant water-cooling flow rate of 6 L.min⁻¹ were used during the welding procedures. The welding current and welding time (Fig. 1) were chosen to produce different weld spots in terms of welding-induced residual stresses profiles. They were set based on previous investigations conducted by Colombo et al.¹⁵ Other welding parameters involved in RSW process were kept constant: electrode force (2 kN), holding time (12 cycles) and squeeze time (32 cycles), being 1 cycle equivalent to the sixtieth part of a second (1 cycle = 1/60 s).

The plastic deformation prior to the RSW process was induced by uniaxially stretching the specimen using a MTS Universal Testing Machine with pneumatic clamping using a pressure of 600 bar, at a cross head speed of 1.0 mm.min⁻¹. Three different engineering strain levels were adopted: 5% (labeled ST5), 10% (ST10) and 15% (ST15). To investigate the influence of the manufacturing route #1 on the integrity of the weld spots, the samples were produced with the welding parameters set RSW2 (Fig. 1). To simulate the bake treatment, the spot-welded samples were produced with two different welding sets: RSW1 and RSW2 (Fig. 1). The samples were subjected to a heat treatment at a temperature of 220°C and a soaking time of

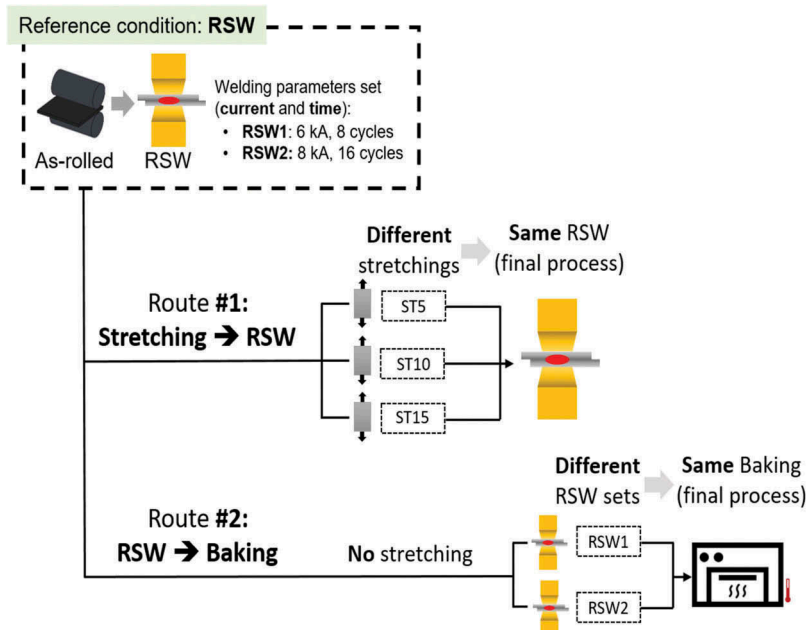


Figure 1. Schematic diagram of manufacturing routes.

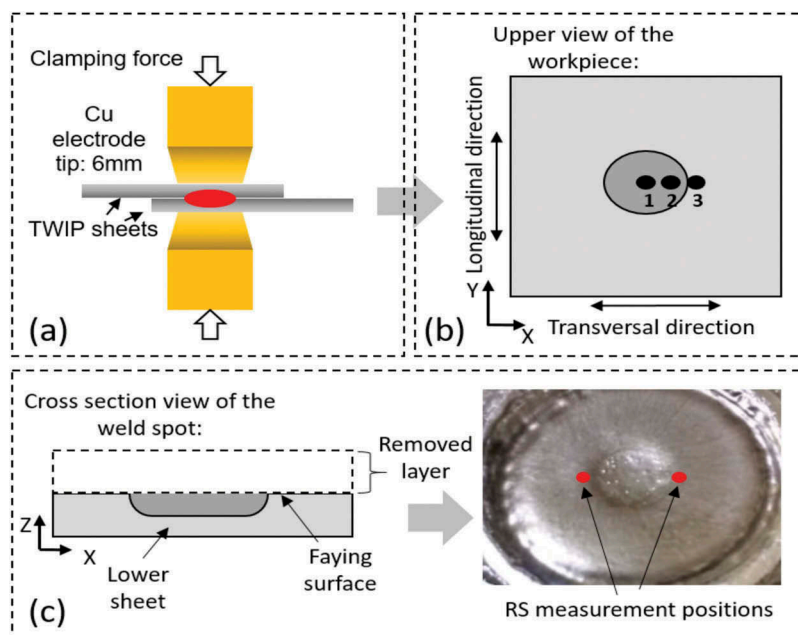


Figure 2. Schematic diagram of: (a) resistance spot welding setup, (b) RS measurement positions on the surface and (c) measurement positions at the core of the weld spots.

30 min and then left to cool down at air. The temperature was monitored by thermocouples attached to the weld spots.

To investigate the work hardening distribution along the cross-section of the weld spots, Vickers hardness maps were produced on polished samples obtained from the reference and from the ST+RSW conditions. The sample preparation was conducted following conventional metallographic procedures. A constant indentation load of 1 N and grid spacing of 62.5 μm were used between each indentation.

The residual stresses (RS) along the weld spots were measured by the X-ray diffraction (XRD) technique, through the $\sin^2\psi$ method^[8], using a Stresstech Xstress3000 – G2R diffractometer. The stress measurements were performed with an X-ray source of Cr-K α and the austenite diffraction plane was (211) plane with a 2θ value of 128.8°, using a collimator diameter of 2 mm. The “peak shift” method has been considered for computing the measured strain into stresses.^[8] Based on the findings of Moshayedi and Sattari-Far^[9], that found the longitudinal residual stresses are the most significant principal stresses in weld spots, only the longitudinal stresses were considered for the discussions in the present study. The measuring points were distributed along the surface and at the core of the specimen, starting at the center of the weld spot toward the edge of the specimen (points 1 to 3, Figs. 2b,c). The layer removal for XRD measurements at the core of the weld spots was conducted by electropolishing, using a Buehler Electromet 4 machine. For each manufacturing condition, five measurements were performed at each point. The average RS values and their respective standard deviations were considered for the discussions.

Results and discussion

Residual stresses induced by the manufacturing route #1

Figure 3 shows the effect of the prior plastic deformation on the residual stresses (RS) profiles along the surface of the weld spots.

It is observed that the highest RS values are found near the edge of the electrode-to-sheet contact (point 2, Fig. 3a), independently of the processing condition. The manufacturing chain has a considerable effect when one observes the entire RS profile along the surface. Different prior plastic deformations induce a meaningful effect on the maximum tensile residual stresses (point 2) along the surface after the welding process.

When a pre-stretching of 5% is applied prior to the RSW stage (Fig. 3(b)), it is observed an increase of around 172 MPa in the maximum RS. The observed increase is of 211 MPa when a pre-stretching of 10% is considered. The maximum RS found is 727 MPa when a plastic strain of 15%, which corresponds to an increase of 237 MPa when compared to the maximum RS found if solely the RSW process is considered. Although a plastic deformation prior to the RSW affects the magnitude of the RS along the weld spot surface, the shape of the RS profile is defined by the RSW process. It is observed in Fig. 3 that the RS increases from the center (point 1) toward the edge of the weld spot (point 2), and then decreases again (point 3), independently on the manufacturing chain prior to the RSW process.

It is observed that the transitions from the RS at point 2 to point 3 are also influenced by the prior plastic deformation. Considering the samples with no prior stretching, the RS drop ($\Delta\text{RS}_{2\rightarrow 3}$) from +463 MPa at point 2 to +234 MPa at point 3, which corresponds to a RS drop of 229 MPa. The $\Delta\text{RS}_{2\rightarrow 3}$ then decreases when a strain hardening is applied prior to the RSW step. For a pre-stretching of 5%, the $\Delta\text{RS}_{2\rightarrow 3}$ is 123 MPa. When a pre-stretching of 10% or 15% is applied, the $\Delta\text{RS}_{2\rightarrow 3}$ is around 50 MPa.

The geometrical discontinuities between points 2 and 3 due to the localized plastic deformation induced by the electrodes are stress concentration sites.^[10] The deteriorating effect of such stress concentration sites to the mechanical reliability of the weld spots may be enhanced by their coexistence with high

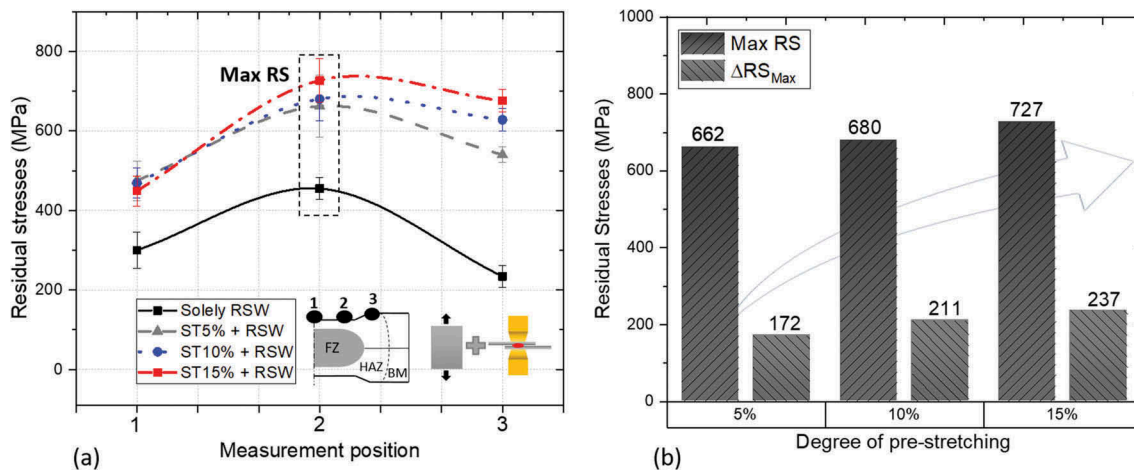


Figure 3. Effect of the manufacturing route #1 on: (a) distributions of residual stresses along the surface of the weld spots and (b) maximum RS found and increase in maximum RS when compared to the solely RSW condition.

tensile residual stresses. According to Zhang and Senkara^[10], the HAZ is the most severely loaded part of a weld spot. The combination of high external loads, stress concentrators and welding-induced residual stresses may thus promote local yielding in these favored sites, enhancing their potential as primary failure sites.

Figure 4a shows the effect of prior plastic deformation on the RS at the core of the weld spots (region near the geometrical notch, Fig. 2c). Considering solely the RSW process, the maximum tensile RS found at the core of the weld spot is 179 MPa, which corresponds to a value of 281 MPa lower than the maximum RS found at the same position on the surface of the weld spots. A possible explanation involves the time that the material layers are exposed to high temperatures: when the welding

current is ceased, the material layers closer to the interface between the workpiece and the electrodes are the first to cool down due to the action of the water-cooled copper electrodes. The inner material layers are, therefore, exposed to higher temperatures for longer times than the outer layers. Colombo et al.^[5] showed that longer welding times facilitate material softening in TWIP steel weld spots. Such softening is manifested by the increase in annealing twins along the HAZ. It also comes accompanied by smoother hardness gradients and lower tensile residual stresses. It should be expected that the longer exposure times of the inner material layers to high temperatures enhance the material softening and the residual stress relaxation. It is in agreement with the lower RS values found at the core of the weld spots shown in Fig. 4a.

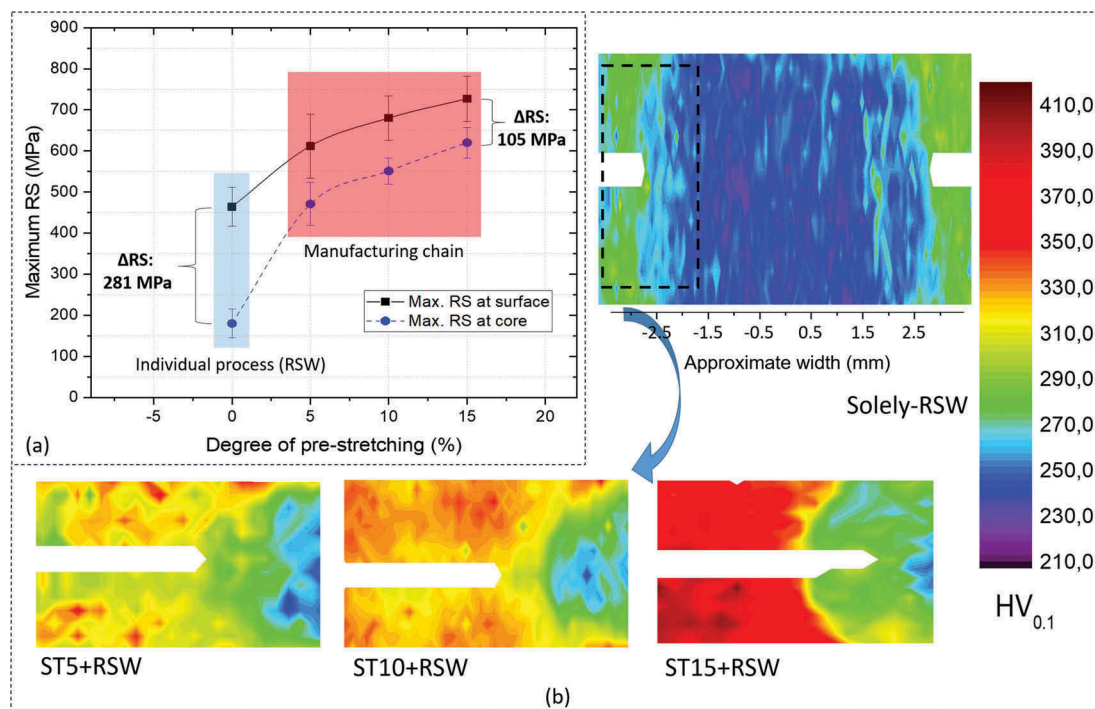


Figure 4. The influence of the manufacturing route #1 on: (a) residual stresses plot and (b) hardness maps.

Similar to the observed for the RS along the surface (Fig. 3), the RS values at the core of the weld spots increase when increasing the prior plastic deformation. When a pre-stretching of 5% is applied (Fig. 4a), the RS is 468 MPa, which corresponds to an increase of 161% in the magnitude of the tensile RS at the same position when solely the RSW is considered. By applying a pre-stretching of 10% or 15%, the RS found are 547 MPa and 620 MPa, respectively.

The increase in the maximum tensile RS with increments of prior plastic deformation can be explained by observing the hardness maps in Fig. 4b. Details of the different grain structures resulting from the RSW cycle can be found in the studies of Colombo et al.^[5] and Tutar et al.^[11] When considering solely the RSW process, it is observed that the hardness distribution is smooth between the BM and the HAZ (dotted square) and it is difficult to distinguish the two regions through the hardness map. The lowest hardness values are found within the region corresponding to the fusion zone (as-cast structure), independently on the manufacturing condition. Such distribution of hardness along the BM and the HAZ is also sensitive to the manufacturing conditions. When applying a prior processing stage involving plastic deformation, it is observed an intense hardness transient between BM and HAZ (material mismatch). The material mismatch intensifies as higher is the prior plastic deformation. When a pre-stretching of 15% is applied, the hardness suddenly drops from around 400 HV along the BM to around 280 HV along the HAZ.

The transition between the BM and the HAZ coincides with the existence of the geometrical notch due to the sheets overlapping, which may enhance the stresses concentration at this site. Such a difference in plastic straining between the BM and the HAZ may be accompanied by plastically induced stresses, according to Withers and Bhadeshia.^[3] The plastic deformation of TWIP steels is characterized by the nucleation and growth of mechanical twins, as evidenced by De Cooman et al.^[1] According to Withers and Bhadeshia^[3] and Laughlin and Hono^[12], mechanical twins are micro stresses sources, as they are displacive transformations that come accompanied by changes in the crystal structure. During the heating period, the expanding FZ also compresses the surrounding material (HAZ), as the HAZ has its plastic flow restricted by the BM.

On the other hand, during the cooling period, the FZ contraction pulls the surrounding material volume, imposing tensile stresses.^[10] Consequently, the harder the base material, the stronger the constraining effect to the HAZ plastic flow. It is expected to enhance the locked-in (residual) stresses that arose from the welding cycle.

When a prior manufacturing stage that involves plastic deformation is considered, the weld spots are prone to RS that arise from at least three different mechanisms: (i) an intensified material mismatch at the region between the BM and the HAZ; (ii) the stronger constraining effect of the BM to the plastic flow of the HAZ and (iii) a higher density of crystalline defects which are sources of micro-scale RS. According to Withers and Bhadeshia^[3] and Rego et al.^[7], as the macro RS are related to the intensity of RS in a micro scale, they should be also higher as more intense is the material mismatch at the region adjacent to the weld spot. It is in agreement with the increase in tensile residual stresses with increments in the prior plastic deformation, as shown in Figs 3a and 4a.

Figure 5 shows the effect of the manufacturing route #1 on the characteristic XRD peaks. The data were obtained from the diffracted peaks at the core of the weld spots. It is observed that a prior plastic deformation tends to broaden the XRD peaks (Fig. 5a). It reflects in an increase of the full width at half maximum (FWHM) values of the XRD peaks with increasing the prior plastic deformation (Fig. 5b). According to Vashista and Paul^[13], the FWHM of the XRD peaks is sensitive to the variation in microstructure and accumulation of lattice disorder in the material, which in turn is affected by any individual processing stage. As shown in Fig. 5b, the FWHM values increase almost linearly with the increase in prior plastic deformation. When a pre-stretching of 15% is applied, the FWHM value is around 30% higher than when solely the RSW process is considered. It may be interpreted as an indicator that the heating cycle during the RSW stage does not reduce the density of crystalline defects induced by the prior plastic deformation. As the TWIP steels are characterized by their plastic flow induced by mechanical twinning, which is a displacive transformation, it is plausible to suppose that the dislocation and twins density at the material fraction adjacent to the FZ is higher as higher is the prior plastic deformation, thus inducing

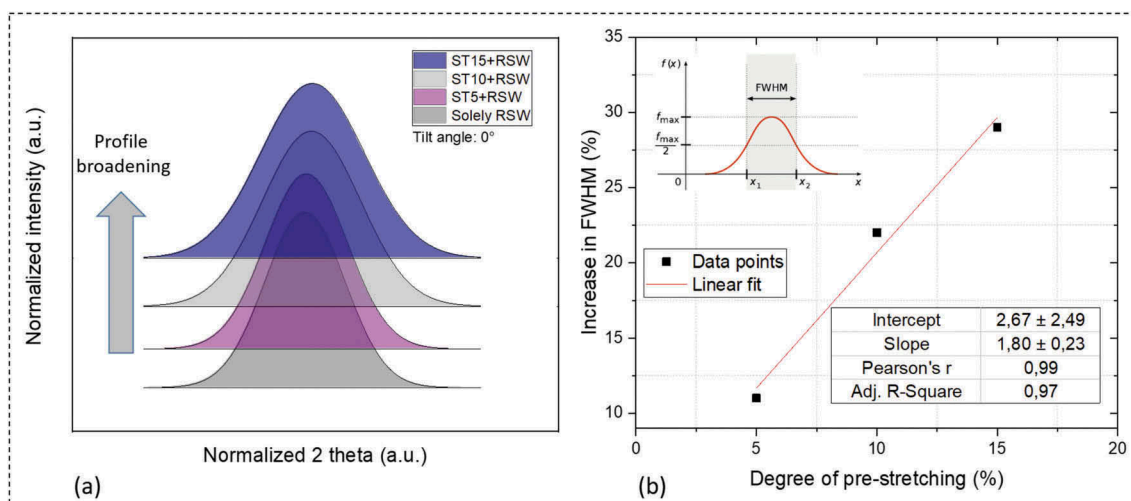


Figure 5. The influence of the manufacturing route #1 on: (a) Gauss fit of XRD peaks and (b) FWHM.

more tensile RS levels. These evidences support the hypothesis of the contribution of the crystalline defects to the increase in the RS, as observed in Fig. 4a.

As shown in Fig. 4a, the maximum RS values are found at the surface, independently of the manufacturing condition. An explanation for this observation is that, besides the thermal effect due to the welding cycle, the outer material layers are subjected to the effect of the mechanical loads induced by the electrodes. Colombo et al.^[5] showed that the compression forces induced by the electrodes are sufficient to induce strain hardening, especially at the material layers closer to the surface. According to Withers and Bhadeshia^[3], both thermal and mechanical loads induce disturbances on the material crystalline lattice and thus affect the RS state. Their combined effect on the outer material layers plus shorter exposure times to high temperature (hindering the onset of softening mechanisms) induce higher tensile RS, which is in agreement with the observations in Fig. 4a.

Due to the fact that the prior plastic deformation affects the material in a global manner, it also affects the differences in magnitude of tensile RS values between the core and the surface. Considering solely the RSW process, Fig. 4a shows that the difference between the maximum RS at core and on the surface is around 281 MPa. When a prior plastic deformation is applied, it is observable that the difference diminishes to 105 MPa and tends to remain constant, independently of the prior plastic deformation applied. As evidenced by the peak broadening and the increase in FWHM magnitude (Fig. 5), it is plausible to presume that the disturbance in crystalline lattice induced by the prior plastic deformation remains within the material. The higher density of crystalline defects at the inner material layers leads to RS levels that tend to approach the ones found on the surface of the weld spots.

Influence of the manufacturing route #2

To investigate if the manufacturing route #2 affects the final residual stresses state, the RSW process parameters were intentionally adjusted to provide two distinct RS profiles (RSW1 and RSW2, Fig. 1). XRD measurements were performed along the surface of the weld spots, as the magnitude of the residual stresses on the surface showed to be the highest (Fig. 4a). The effect of the baking treatment on the RS state along the surface of the weld spots is shown in Fig. 6. When considering solely the RSW process, it is observed that the RS profiles are remarkably sensitive to the welding parameters. While the parameters set RSW1 induce an inhomogeneous RS gradient, with an abrupt decrease in RS from point 2 to point 3, RSW2 exhibits a smoother RS gradient along these different positions.

When the weld spots are subjected to a post-weld baking treatment stage, it is observed a tendency of RS relaxation along the RS profiles. The maximum tensile RS before baking was 527 MPa for the welding parameters set RSW1. After a bake treatment of 220°C during 30 min, the maximum tensile RS decreased to 449 MPa. It corresponds to a relaxation of tensile RS of 78 MPa. A shift of the RS profile toward lower values is also observed for the welding parameters set RSW2. When observing the RS values before and after the BT stage for each individual measurement point, it is noticeable that, the higher the RS magnitude, the higher is the RS relaxation induced by the BT stage.

The data in Fig. 6 suggest that the magnitude of the RS along the weld spots is also sensitive to the manufacturing route #2. Although the RS values differ from the as-welded to the post-heat treated condition, the RS profile seems to be defined by the RSW process. It is also worth to note that the

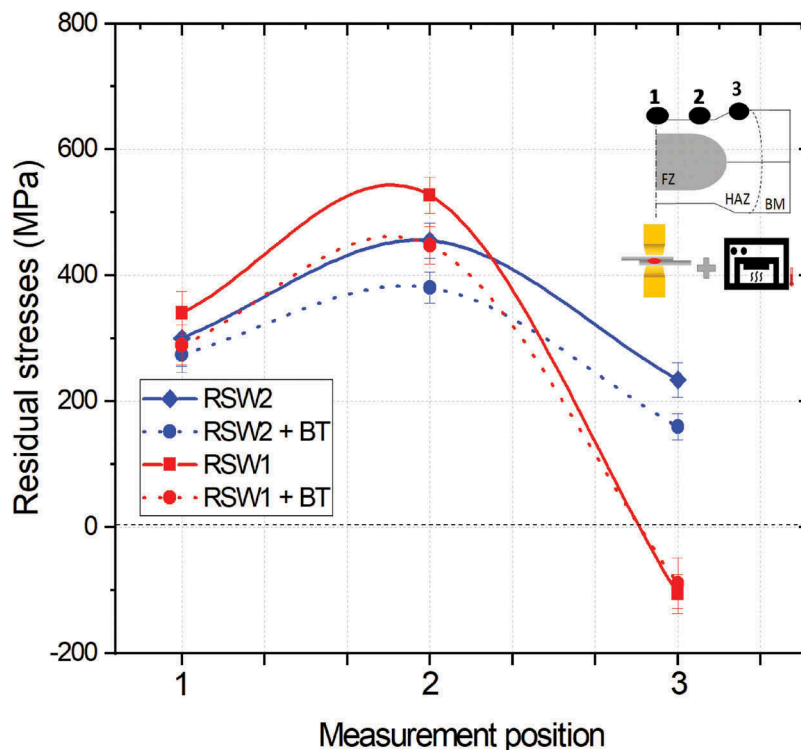


Figure 6. Effect of manufacturing route #2 on the RS profiles along the surface.

steep RS transient from point 2 to point 3 is not altered by the post-weld heat treatment, when the welding parameters are set as RSW1. Considering solely the RSW process, the RS decreases from +527 MPa at point 2 to around -106 MPa to point 3, which corresponds to a RS drop of 633 MPa. When the manufacturing chain is considered, the RS decreases from +449 MPa to around -90 MPa, which corresponds to a RS drop of 539 MPa. It is still a steep RS gradient, as it corresponds to 89% of the yield stress of the TWIP980 steel, which is 601 MPa, according to Joo and Huh.^[14] When the RSW cycle is adjusted to provide a smoother RS transition (welding set RSW2), the RS profile induced by the RSW is also retained after the bake treatment, as seen in Fig. 6. The data in Fig. 6 indicate that the same bake treatment is not effective in generating the same stresses state to the different welding parameters set, evidencing the relevance of the entire manufacturing chain. According to Huang et al.^[15], the relaxation of RS is a thermally activated process by which the crystalline defects are annihilated and rearranged. For considerably low temperatures, as the ones involved in a bake treatment, which are far below $0.4xT_f$ (material *liquidus* temperature), these conversions may occur mainly by deformation micromechanisms, such as rearrangement of dislocations, etc. Softening and relaxation mechanisms which could significantly alter the dislocation density at higher scale, such as recrystallization, are not expected to occur at such temperatures.

Conclusions

- The higher the plastic deformation applied prior to the RSW stage, the higher is the hardness mismatch from the BM toward the FZ.
- The higher the plastic deformation applied prior to the RSW stage, the more tensile is the post-weld residual stresses both at the core and surface of the weld spots.
- The post-weld baking-treatment-induced relaxation of residual stresses, but the residual stresses profiles induced by the RSW stage are maintained after the baking treatment (final process).
- Independently of the prior and post-weld manufacturing stages, the residual stresses profiles are determined by the RSW process.
- The findings from this study reinforces the relevance in considering the effect of a manufacturing chain on the performance of a component instead of taking into account solely individual processes.

Article Highlights

- The magnitude of the post-weld residual stresses has positive correlation to the degree of plastic deformation prior to the RSW process.
- The steep residual stresses gradients induced by the RSW are preserved after the post-weld bake treatment.
- Both prior stretching and post-weld baking treatment modify the residual stresses state, but the residual stresses profiles showed to be defined by the RSW stage.

Acknowledgments

Authors would like to acknowledge the *Laboratório de Estruturas Leves* (LEL) from the *Instituto de Pesquisas Tecnológicas do Estado de São Paulo* (IPT), especially in the person of Mario Batalha, for the support with the XRD measurements. The authors also thank the funding of the *Coordenação de Aperfeiçoamento de Pessoal de Nível Superior* (CAPES) the *Brazilian agency* (CNPq) under grant 306193/2017-5.

Funding

This work was supported by the Conselho Nacional de Desenvolvimento Científico e Tecnológico [306193/2017-5].

References

- [1] De Cooman, B. C.; Estrin, Y.; Kim, S. K. Twinning-induced plasticity (TWIP) steels. *Acta Mater.* **2018**, *142*, 283–362. DOI: [10.1016/j.actamat.2017.06.046](https://doi.org/10.1016/j.actamat.2017.06.046).
- [2] Zavattieri, P. D.; Savic, V.; Hector, L. G.; Fekete, J. R.; Tong, W.; Xuan, Y. Spatio-temporal characteristics of the portevin-le chatelier effect in austenitic steel with twinning induced plasticity. *Int. J. Plast.* **2009**, *25*(12), 2298–2330. DOI: [10.1016/j.ijplas.2009.02.008](https://doi.org/10.1016/j.ijplas.2009.02.008).
- [3] Withers, P. J.; Bhadeshia, H. K. D. H. Residual stress. Part 2 – nature and origins. *Mater. Sci. Technol.* **2001**, *17*(4), 366–375. DOI: [10.1179/026708301101510087](https://doi.org/10.1179/026708301101510087).
- [4] Tamizi, M.; Pouranvari, M.; Movahedi, M. Welding metallurgy of martensitic advanced high strength steels during resistance spot welding. *Sci. Technol. Weld. Join.* **2017**, *22*(4), 327–335. DOI: [10.1080/13621718.2016.1240979](https://doi.org/10.1080/13621718.2016.1240979).
- [5] Colombo, T. C. A.; Rego, R. R.; Otubo, J.; de Faria, A. R. Mechanical reliability of twip steel spot weldings. *J. Mater. Process. Tech.* **2019**, *266*, 662–674. DOI: [10.1016/j.jmatprotec.2018.11.021](https://doi.org/10.1016/j.jmatprotec.2018.11.021).
- [6] Kilic, S.; Ozturk, F.; Sigirtmac, T.; Tekin, G. Effects of pre-strain and temperature on bake hardening of TWIP900CR steel. *J. Iron Steel Res. Int.* **2015**, *22*(4), 361–365. DOI: [10.1016/S1006-706X\(15\)30012-1](https://doi.org/10.1016/S1006-706X(15)30012-1).
- [7] Rego, R.; Löpenhaus, C.; Gomes, J.; Klocke, F. Residual stress interaction on gear manufacturing. *J. Mater. Process. Technol.* **2018**, *252* (April 2017), 249–258. DOI: [10.1016/j.jmatprotec.2017.09.017](https://doi.org/10.1016/j.jmatprotec.2017.09.017).
- [8] Hauk, V.; *Structural and Residual Stress Analysis by Nondestructive Methods*; Elsevier: Amsterdam, **1997**.
- [9] Moshayedi, H.; Resistance Spot, S.-F. I. Welding and the effects of welding time and current on residual stresses. *J. Mater. Process. Technol.* **2014**, *214*(11), 2545–2552. DOI: [10.1016/j.jmatprotec.2014.05.008](https://doi.org/10.1016/j.jmatprotec.2014.05.008).
- [10] Zhang, H.; Senkara, J. *Resistance Welding: Fundamentals and Applications*, 2nd ed.; CRC Press: Boca Raton, **2011**.
- [11] Tutar, M.; Aydin, H.; Bayram, A. Effect of weld current on the microstructure and mechanical properties of a resistance spot-welded TWIP steel sheet. *Metals (Basel)*. **2017**, *7*. DOI: [10.3390/met7120519](https://doi.org/10.3390/met7120519).
- [12] Laughlin, D. E.; Hono, K. *Physical Metallurgy, Vol. I*, 5th ed.; Elsevier B.V.: Amsterdam, **2014**.
- [13] Vashista, M.; Paul, S. Correlation between full width at half maximum (FWHM) of XRD peak with residual stress on ground surfaces. *Philos. Mag.* **2012**, *92*(33), 4194–4204. DOI: [10.1080/14786435.2012.704429](https://doi.org/10.1080/14786435.2012.704429).
- [14] Joo, G.; Huh, H. Modeling of rate-dependent hardening behaviors of the TWIP980 steel sheet in tension and compression. *Procedia Eng.* **2017**, *207*, 143–148. DOI: [10.1016/j.proeng.2017.10.752](https://doi.org/10.1016/j.proeng.2017.10.752).
- [15] Huang, J.; Zhang, K. M.; Jia, Y. F.; Zhang, C. C.; Zhang, X. C.; Ma, X. F.; Tu, S. T. Effect of thermal annealing on the microstructure, mechanical properties and residual stress relaxation of pure titanium after deep rolling treatment. *J. Mater. Sci. Technol.* **2019**, *35*(3), 409–417. DOI: [10.1016/j.jmst.2018.10.003](https://doi.org/10.1016/j.jmst.2018.10.003).